Regular Article

ANALYTICAL AND BIOANALYTICAL CHEMISTRY RESEARCH

Published by the Iranian Chemical Society

Anal. Bioanal. Chem. Res., Vol. 9, No. 3, 259-268, July 2022.

An Electrochemical Sensor Based on Poly(methyl orange) Modified Glassy Carbon Electrode for Simultaneous Determination of Vitamins B_2 and C in Aqueous Solution

Mohamed Abd-Elsabour*, Keriman M. Abd-Elsabur, Fawzy H. Assafand and Ibrahem M.A. Hasan

Faculty of Science, Chemistry Department, South Valley University, Qena, 83523, Egypt

(Received 22 September 2021 Accepted 9 January 2022)

A selective and sensitive voltammetric sensor was constructed using a Poly(methyl orange)/glassy carbon electrode (PMO/GCE). The PMO/GCE sensor was applied to investigate the electrochemical behavior of ascorbic acid (AA) and vitamin B_2 (VB_2) in the PBS buffer solution. The sensor was applied for the individual and simultaneous determination of AA and VB_2using cyclic and differential pulse voltammetry (DPV) techniques. Different experimental parameters including scan rate (25-500 mV s^{-1}), pH (4-8 for AA and 3-10 for VB_2) and analyte concentration (10-40 µM for AA and 4-85 µM for VB_2) have been studied and optimized. High electrocatalytic activities for oxidation of AA and VB2 were performed with pH values of 7.0 and 6.0, respectively. In addition, the results indicated that the oxidation process of AA and VB_2 was under diffusion control. The detection limits, quantitation limits and linear ranges were 0.575, 1.916 and 10-40 µM for AA and 0.922, 3.073 and 5-85 µM for VB_2, respectively, under the optimized DPV conditions. Peak separation of AA from VB_2 was 660 mV which is enough to determine these vitamins simultaneously. The fabricated sensor has been applied successfully for estimation of AA and VB_2 in real samples with good selectivity, stability and reproducibility.

Keywords: Ascorbic acid, Riboflavin, Electropolymerization, Methyl orange, Cyclic voltammetry, Differential pulse voltammetry

INTRODUCTION

Ascorbic acid (AA) also called widely as vitamin C, is an important vitamin in the human diet. AA is used for infections such as gum disease, bronchitis, acne and other skin infections [1]. Also, it has been frequently used to prevent and treat influenza, common cold, mental illness and infertility [2,3]. Riboflavin (vitamin B_2, VB_2) is a significant vitamin that stimulates biological reactions of carbohydrates, proteins and fats in the human body. VB_2 is used for preventing inflammation of the mouth, lips, and tongue. It also helps to improve visibility and reduce eye fatigue [4]. Besides, it's very essential for the metabolism of amino acids and for the maintenance body [5].

Several analytical techniques for measuring AA and VB_2 have been studied including high-performance liquid chromatography [6,7], spectrophotometry [8], capillary electrophoresis [9], chemiluminescence [10] and electrochemical methods [11-13]. The electrochemical techniques are widely used due to their high selectivity, stability, sensitivity, rapidity and accuracy [14,15].

Methyl orange (MO) is an anionic terminated azo dye that mediates the reactions of electron and proton transfer. The presence of functional groups like $N(CH_3)_2$, –N=N– and $–SO_3H$ is responsible for electrochemically active properties of MO [16,17]. MO has been electrochemically polymerized to detect some analytes including L-dopa, 4-nitrophenol, vanillin, and amodiaquine drug [17-20]. However, no study was published for electrochemical detection of AA or VB_2 using poly(methyl orange) (PMO).

In the present study, a film of PMO was fabricated at a glassy carbon electrode (GCE) using cyclic voltammetry

*Corresponding author. E-mail: m.sabour28@sci.svu.edu.eg

(CV) technique. The obtained sensor was applied for electrochemical determination of AA and VB_2. Various experimental parameters were optimized for the simultaneous determination of the two vitamins in real samples with low detection limit, good sensitivity and high anti-interference ability.

EXPERIMENTAL

Apparatus

All experiments were done using apparatus EG&G Princeton applied research POTENTIOSTAT/ GALVANOSTAT (model 263, USA) which connected with an external computer. The electrochemical cell (model k0264 micro-cell) consists of three electrodes: an Ag/AgCl saturated KCl (model k0265) serves as the reference electrode. While, the counter electrode (model k0266) is a high purity platinum wire and an electrochemically modified GCE (2 mm diameter, ALS Co., Ltd.) acts as the working electrode. A Cyber Scan pH 500 Meter (Euteoh-India) was used to adjust pH values. The structure morphology of the fabricated electrode was examined using a field-emission scanning electron microscope (FE-SEM, QUANTA FEG250).

Chemicals and Solutions

All chemicals used in the experiments were of analytical reagent grade unless otherwise specified and used without further purification. Stock solutions of 0.01 M vitamins B_2 and C (Aldrich Chemical Co. Ltd.) were prepared by dissolving the appropriate amounts in bi-distilled water. The PBS was made from $NaH_2PO_4.H_2O$ (El Nasr Pharm. Chem. Co (ADWIC), 98% purity) and was used as a supporting electrolyte. Solutions of 1.0 M NaOH and 1.0 M HCl were used to adjust the pH. All solutions were freshly prepared with bi-distilled water, and all experiments were carried out at room temperature (25 °C).

Fabrication of the PMO/GCE

Before modification, the GCE was first polished with a smooth polishing cloth and alumina slurry (0.05 µm), followed by sonication in nitric acid, acetone and cleaned with distilled water. The clean GCE was immersed in 0.1 M PBS (pH 7.0) containing 5.0 mM of MO monomer. Then, the working electrode was electro-polymerized by cycling potential between -0.25 to 1.25 V (*vs*. Ag/AgCl) at a scan rate of 100 mV s^{-1} for 10 cycles. Finally, the modified electrode was carefully cleaned with deionized water to remove unreacted particles.

Real Samples Preparations

Fresh citrus juices (orange, lemon) were obtained using a mechanical squeezer. The resulting juices were filtered *via* normal filter paper and centrifuged. Finally, 1.0 ml of the filtrate was added to 100 ml of 0.1 M PBS (pH 7.0) in a voltammetric cell. The standard addition method was used to evaluate the amounts of vitamin C in the samples. For tablets, an accurately weighed portion of the homogeneous powder sample obtained from one tablet (equivalent to 500 mg AA) dissolved in 100 ml deionized water, then filtrated. Finally, a different volume of the solution was transferred to a voltammetric cell containing 0.1 M PBS (pH 7.0).

Also, the standard addition method was used for the determination of VB_2 in various real samples. For cow milk purchased from a local supermarket, 1.0 ml of glacial acetic acid was added to 5.0 ml of the sample to precipitate out the proteins. Then, the solution was digested for 20 min in a water bath and centrifuged for 10 min. Finally, 1.0 ml of the homogenous solution was added to 100.0 ml of 0.1 M PBS (pH 6.0) in a voltammetric cell. As for a multivitamin tablet (1.3 mg VB_2), each tablet was weighed, carefully crushed, and dissolved in 25.0 ml of 0.1 M PBS (pH 6.0). While 10.0 ml of riboflavin syrup was directly diluted with 0.1 M PBS (pH 6.0).

RESULT AND DISCUSSION

Electropolymerization of MO at the GCE Electrode

The OM was electropolymerized within the potential range of -0.25 to 1.25 V (c. Ag/AgCl) for 10 cycles. Figure 1 shows CVs of 5.0 mM MO in 0.1 M PBS (pH 7.0) at a scan rate of 100 mV s^{-1}.

The CV curves show two oxidation peaks at 0.33, 0.77 V, and a reduction peak at 0.18 V. The peak at a potential 0.77 V is the result of the oxidation of MO monomer. Meanwhile, the redox peaks are related to the formation of PMO film [18]. In addition, the second

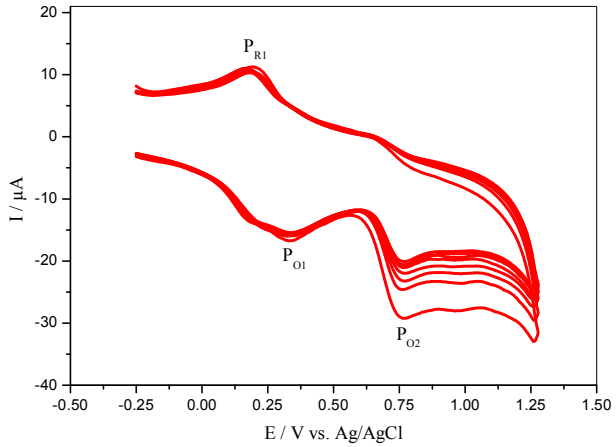

Fig. 1. CVs of 5mM MO in 0.1 M PBS (pH7.0), potential from -0.25 to 1.25 V (*vs*. Ag/AgCl) at a scan rate at 100 mV s^{-1}.

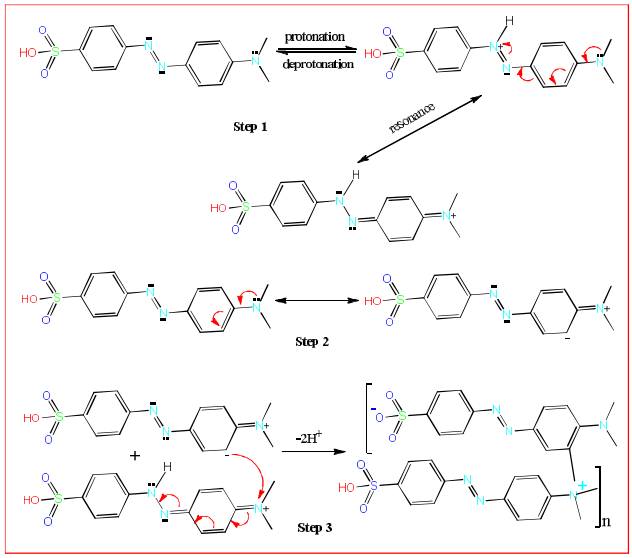

Scheme 1. The possible reaction mechanism of the electropolymerization of MO on the GCE surface

oxidation peak current is gradually increased with increasing the cycle number. This indicates the growth of PMO film *via* redox reaction on the surface of GCE [21,22]. According to the above results and literature [16], the possible reaction mechanism may be as Scheme 1.

The CVs of 0.1 M KNO_3 in the presence of 3.0 mM $K_3[Fe(CN)_6]$ at the PMO/GCE at different scan rates (100-1000 mV s^{-1}) were measured. Then, the anodic current I_p is plotted against the square root of the scan rate as shown in Fig. 2. The slope of the resulting straight line (Ip = 4.517 v1/2 0.657, R2 = 0.9912) was replaced by the following Randles-Sevcik equation [23-25]:

$$Ip = 0.446nFAC(nFDv/RT)^{1/2}$$

where n is the number of electrons (for this system n = 1), C is the concentration of the electroactive species (mM), A is the electroactive surface area (cm^2), D is the diffusion coefficient (cm^2 s^{-1}); 5.6 × 10^{-6} cm^2 s^{-1}, and other symbols have the usual meanings. The calculated value for PMO/GCE was 0.22 cm^2, which is greater than the bare GCE (0.126 cm^2).

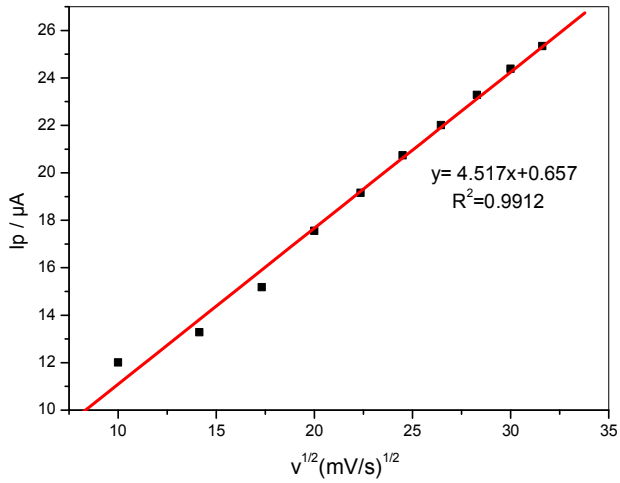

Fig. 2. The plot of I_p against the square root of the scan rate.

Voltammetric Behavior of AA and VB_2 at the PMO/GCE

The electro-catalytic responses of the PMO/GCE towards AA and VB_2 were investigated with the CV method. Figure 3A depicts the CVs of PMO/GCE in the absence of AA and in the presence of 0.1 mM AA (0.1 M PBS, pH 7.0, and scan rate 100 mV s^{-1}) at bare GCE (curve b) and PMO/GCE electrodes (curve c). No peaks were observed in the absence of AA at bare, and PMO modified electrodes (curve a). An oxidation peak close to 0.24 V and no reduction peaks were observed (curve b)

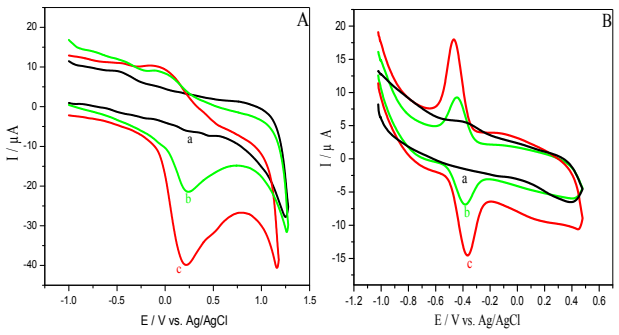

Fig. 3. A) CVs of 0.1 M PBS (pH 7.0) at the PMO/GCE without AA (a), at the bare GCE in 0.1 mM AA (b) and at the PMO/GCE in 0.1 mM AA (c) with a scan rate 100 mV s^{-1}. B) CVs of 0.1 M PBS (pH 6.0) at the PMO/GCE without VB_2 (a), at the bare GCE in 0.5 mM VB_2 (b) and at the PMO/GCE in 0.5 mM VB_2 (c) with a scan rate 50 mV s^{-1}.

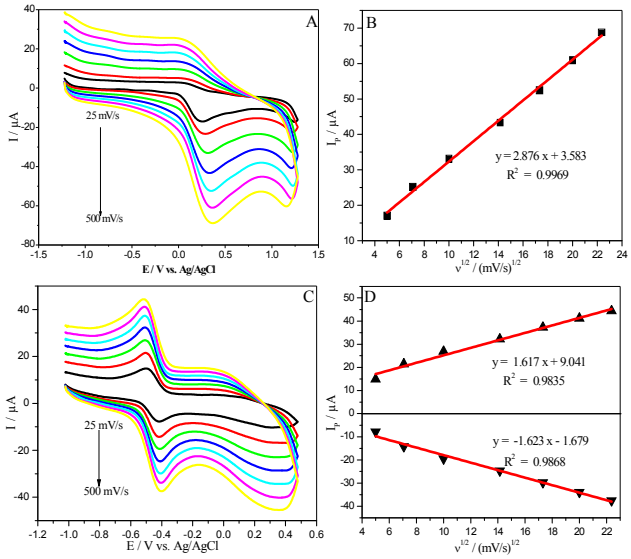

Fig. 4. CVs of the PMO/GCE in 0.1 M PBS (pH 7) at a series of scan rates (25, 50, 100, 200, 300, 400 and 500 mV s^{-1}) for 0.1 mM of AA (A) and for 0.5 mM of VB_2 (C) and the peak current (I_p) as a function of the square root of the scan rate ($\nu^{1/2}$) for AA (B) and VB_2 (D).

indicating the irreversible oxidation of AA at the bare GCE. The peak potential was shifted to a more negative value (E_p = 0.21V) and the current increased three times by using the PMO/GCE (curve c) due to the high electron transfer rate.

Similarly, the electrochemical behavior of VB_2 (0.1 M PBS, pH 6.0, and scan rate 50 mV s^{-1}) was studied using CVs, as shown in Fig. 3B. Where the curve (a) at the PMO/GCE without VB_2 and the curves (b) and (c) represent the CVs of 0.5 mM VB_2 at the bare GCE and PMO/GCE, respectively. The bare GCE (curve b) gave a low current response with redox peaks emerging at potential -0.38 V and -0.44 V (ΔE_p = 60 mV) indicating that VB_2 undergoes a reversible process with two-electron exchange reactions. The same behavior was observed at the PMO/GCE with higher peak currents than the bare GCE. Finally, there is no measurable peak for the proposed sensor (curve an in Figs. 3A and B) over the potential window studied for PBS as a supporting electrolyte. This makes it clear indicates that the modified GCE acts as a good electrocatalyst for the oxidation of AA and VB_2.

Effect of Potential Scan Rate

The impact of potential scan rate on the electrochemical oxidation of 0.1 mM AA in 0.1 M PBS (pH 7.0) at the PMO/GCE was recorded (Fig. 4A). It can be seen that increasing the scan rate from 25 to 500 mV s^{-1} caused a corresponding rapid increase in the anodic peak current of the AA. Besides, a positive shift in the peak potential was observed due to an irreversible electro-oxidation reaction of AA. Figure 4B shows a linear dependence of the peak current (I_p) of AA on the square root of the scan rate ($\nu^{1/2}$) on the same range. The obtained equation was I_p (µA) = 2.876$\nu^{1/2}$ ((mV s^{-1})$^{1/2}$) + 3.583 with a good correlation coefficient (R^2 = 0.9969). This indicates that the electrochemical oxidation of AA at our modified electrode was diffusion-controlled [26,27].

Figure 4C shows the influence of various scan rates (25-500 mV s^{-1}) on peak current and peak potential of 0.5 mM of VB_2 in 0.1 M PBS at the PMO/GCE. A significant increase in VB2 redox peak current was observed with increased scan rate. In addition, their oxidation and reduction peak potentials were negligibly shifted to more anodic and more cathodic values. The above results showed enhanced reversibility of the electron transfer process of VB_2 on the surface of the PMO/GCE. Herein, both peak currents of VB_2 were linear with the square root of the scan

rate as displayed in Fig. 4D. The plot of I_p *vs.* $\nu^{1/2}$ can be expressed by the equations: I_{pa} (μA) = 1.617$\nu^{1/2}$ ((mV s^{-1})$^{1/2}$) + 9.041 (R^2 = 0.9835) and I_{pc} (μA) = -1.623 $\nu^{1/2}$ ((mV s^{-1})$^{1/2}$) -1.679 (R^2 = 0.9868). This behavior confirmed that both processes on the modified electrode surface are controlled by diffusion rather than adsorption [28,29].

Effect of pH

The effect of pH of PBS as a supporting electrolyte on the electrochemical response of AA and VB2 was investigated. The small amounts of 0.1 M HCl and 0.1 M NaOH solutions were employed to regulate the pH values of the PBS. Figure 5A depicts the CVs of 0.1 mM AA at the PMO/GCE with a scan rate of 100 mV s^{-1} in 0.1 M of PBS with varying pH from 4.0 to 8.0. The change in pH values shows remarkable effects on the oxidative peak current and peak potential of AA. Thus, the peak current decreased with the increase in the pH value from 4.0 to 7.0, and there was a conversely decrease with the continuous increase in pH. This means that the electrocatalytic oxidation of AA at the PMO/GCE has pH 7.0 as the optimal value. Also, Fig. 5B shows a linear shift of the oxidative peak potential towards negative values with an increasing pH with the regression equation of E_p (V) = -0.054 pH + 0.02 (R^2 = 0.9978). A slope of 54 mV is very close to the Nernstian value (59 mV) for a two-electrons and two-protons oxidation process [30,31].

The influence of pH on the 0.5 mM VB_2 in the 0.1 M PBS at the PMO/GCE was investigated at a scan rate of 50 mV s^{-1}. The pH results (3.0 to 10.0) are given in Fig. 5C. It is clear that the redox peak currents decreased considerably with pH increasing to 6.0 due to degradation of VB_2 at a higher pH, as reported by others [32]. At higher pH value, there was a decline in the peak currents. Therefore, the highest current and best peak shape were achieved at pH 6.0 due to the faster electron transfer rate. Therefore, pH 6.0 was chosen for optimal pH in subsequent experiments.

Moreover, the redox peak potentials of RF at the PMO/GCE were shifted linearly to more negative values with increasing the pH. Figure 5D signifies the plot of the redox peak potentials of VB_2 against the pH with the corresponding equations E_{pa} (V) = -0.048 pH-0.073 (R^2 = 0.9881) and E_{pc} (V) = -0.059 pH-0.086 (R^2 = 0.9931). The slopes of 48 and 59 mV/pH are similar to the ideal

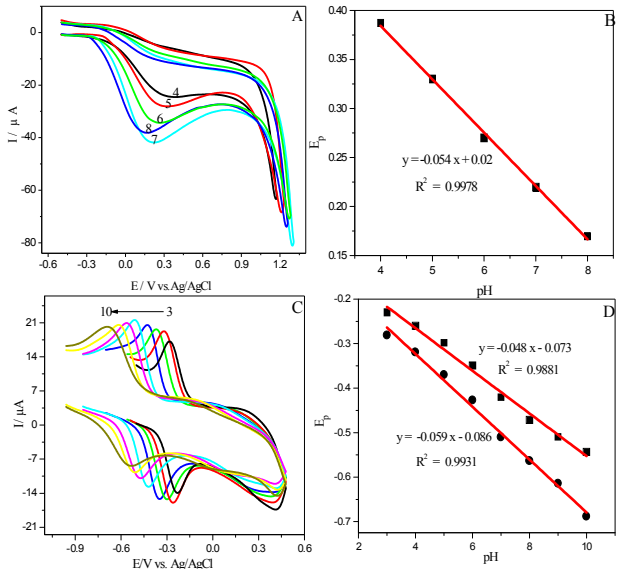

Fig. 5. CVs of the PMO/GCE in 0.1 M PBS with (A) pH range (4.0-8.0) for 0.1 mM of AA at a scan rate 100 mV s^{-1} and (C) pH range (3.0-10.0) for 0.5 mM of VB_2 at a scan rate 50 mV s^{-1}. The peak potential (E_p) as a function of pH for AA (B) and VB_2 (D).

value of 59 mV, indicating that the proton: electron ratio is 1 for both reactions of VB_2.

Voltammetric Determination of AA and VB_2 at PMO/GCE

Differential pulse voltammetry (DPV) was employed for calibration curves studies due to its higher sensitivity and selectivity than CV. Optimum conditions for the DPVs response were established at pulse height 25 × 10^{-3} V, pulse width 50 × 10^{-3} s, step time 0.1 s, and scan rate 20 mV s^{-1}. Figure 6A illustrates the DPVs responses of the PMO/GCE towards AA oxidation in 0.1 M PBS (pH 7.0) with a scan rate of 100 mV s^{-1} at different concentrations. The AA anodic peak current was observed to increase with an increase in its concentration range (10-40 μM), and its potential shifted to more positive values. The corresponding calibration curve was constructed by plotting the anodic peak current *vs.* known AA concentrations, as shown in Fig. 6B. A good linear response was achieved and described as I_P (μA) = 2.066 C (μM) + 11.709 (R^2 = 0.9989). The detection and quantification limits were estimated to be 0.575 and 1.916 μM according to the DL = 3 SD/slope and

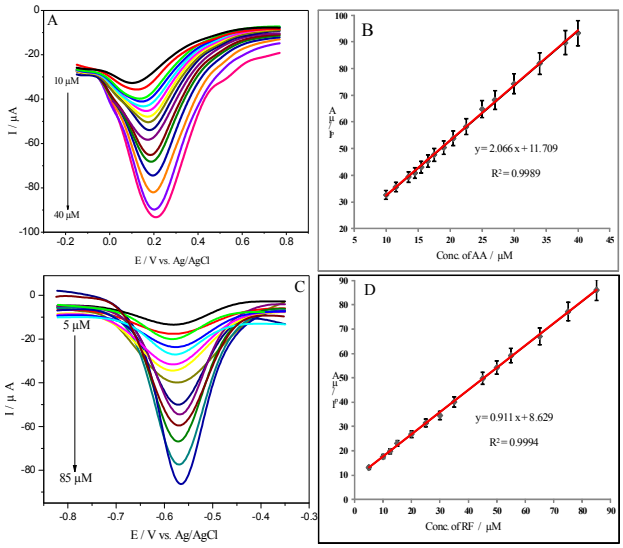

Fig. 6. DPVs of the PMO/GCE (A) in 0.1 M PBS (pH 7.0) containing various concentrations of AA (10.0, 11.5, 13.5, 14.5, 15.5, 16.5, 17.5, 19.0, 20.5, 22.5, 25.0, 27.0, 30.0, 34.0, 38.0 and 40.0 µM) and (C) in 0.1 M PBS (pH 6.0) containing different concentrations of VB_2 (5.0, 10.0, 12.5, 15.0, 20.0, 25.0, 30.0, 35.0, 45.0, 50.0, 55.0, 65.0, 75.0 and 85.0 µM) at pulse High 25×10^{-3} V, pulse width 50×10^{-3} s, step time 0.1 s and scan rate 20 mV s^{-1}. (B) and (D) are the corresponding calibration curves for AA and RF, respectively.

QL = 10 SD/slope definition [33,34], respectively, where SD is the standard deviation of the 16 blanks. 6C represents the DPVs response at the PMO/GCE in 0.1 M of PBS containing various concentrations of VB_2. When the concentration increased from 20.0 to 100.0 µM, the anodic peak current increased continuously and its potential was shifted to more positive values. Moreover, the linear calibration curve was obtained for the measuring range, as shown in Fig. 6D. The corresponding linear equation was I_P (µA) = 0.911 C (µM) + 8.629 with R^2 = 0.9994. Herein, the DL was calculated to be 0.922 µM while the QL was determined to be 3.073 µM. For comparison purposes, analytical methods, detection range, and the detection limit were compared with those of other developed sensors (Table 1). Results show that PMO/GCE modified electrode has a comparable or better performance than many developed sensors with the simplicity of the preparation method.

Simultaneous Electrochemical Sensing of AA and VB_2

The main objective of this work is to simultaneously determine AA and VB_2 at the synthesized sensor in physiological solutions. Figure 7A depicts the DPVs of 0.1 M PBS containing 53.0 µM of VB_2 and different concentrations of AA (10-34 µM) at the PMO/GCE under the optimal conditions. The oxidative peak of VB_2 at -0.47 V is well separated by 660 mV from the AA peak at 0.19 V, allowing the determination of these vitamins simultaneously. In addition, the peak current of AA increased linearly with increasing concentration in the range of (10-34 µM) while the other one of VB_2 kept almost constant. Moreover, the results represented a good

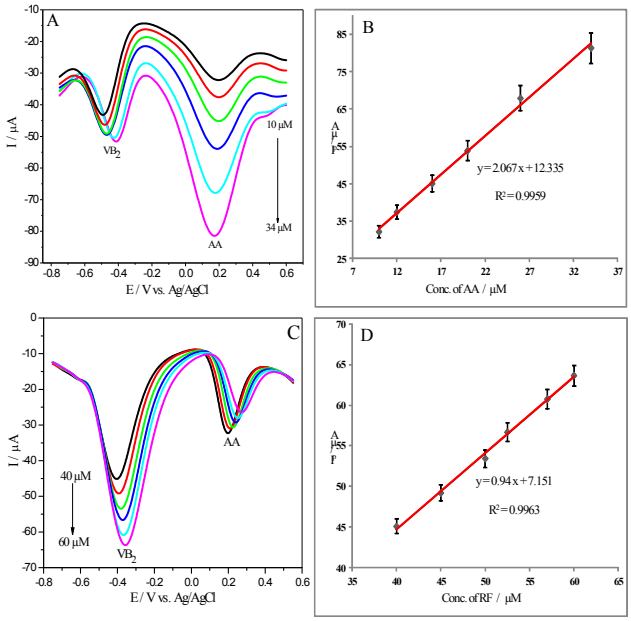

Fig. 7. DPVs of the PMO/GCE (A) in 0.1 M PBS (pH 7.0) containing 53.0 µM of VB_2 and various concentrations of AA (10.0, 12.0, 16.0, 20.0, 26.0 and 34.0 µM) and (C) in 0.1 M PBS (pH 6.0) containing 10.0 µM of AA and different concentrations of VB_2 (40.0, 45.0, 50.0, 52.5, 57.0 and 60.0 µM) at pulse height 25×10^{-3} V, pulse width 50×10^{-3} s, step time 0.1 s and scan rate 20 mV s^{-1}. (B) and (D) are the corresponding calibration curves for AA and RF, respectively.

Table 1. Comparison between the Newly Developed Electrode and other Reported Modified Electrodes

Method	Modified electrode	Analyte	Linear range (μM)	LOD (μM)	Ref.
SWV	GNPs/CPE	AA	1.2-25.0	0.35	[15]
CV	DOH/CPE[a]	AA	3.0-120	0.38	[34]
CV	βCD-ox CNF[b]	AA	100-400	0.9	[38]
DPV	Mn-doped ZnONRs/GO/GCE[c]	AA	500-5500	0.02	[39]
CV	MgB_2-MWCNT/GCE	AA	200-1000	1.3	[40]
DPV	TiO_2NPs/CPE[d]	VB_2	2.4-240	1.6	[31]
DPV	MnO_2/CPE	VB_2	0.02-9.0	0.015	[32]
CV	SLSMCNTPE[e]	VB_2	2.0-200	0.0925	[41]
DPV	PEDOT/$Fe(CN)_6^{4-}$/GCE[f]	VB_2	0.04-200	0.02	[42]
DPV	NPG-modified electrode[g]	VB_2	5.0-250	0.1	[43]
DPV	PMO/GCE	AA VB_2	10-40 5.0-85	0.575 0.922	This work

[a]2,2'-[3,6-Dioxa-1,8-octanediylbis(nitriloethylidyne)]-bis-hydroquinone carbonpaste electrode, [b]β-cyclodextrin/ carbon nano fiber, [c]Mn-doped ZnO nano rods modified grapheme oxide/GCE, [d]TiO_2 nanoparticles modified carbon paste electrode, [e]Sodium lauryl sulfate modified carbon nanotube paste electrode, [f]poly(3,4-ethylenedioxythiophene)/ ferricyanide ($Fe(CN)_6^{4-}$) at glassy carbon electrode, [g]Nanoporous gold at modified electrode.

Table 2. Tolerance Ratios (Concentration which Gave a Relative Error of ±5.0%) of Foreign Species in the Individual Determination of 0.1 mM AA and VB_2 at the PMO/GCE

Interference	Tolerance ratio ($C_{species}/C_{analyte}$)
Na^+, K^+, Mg^{2+}, Cl^-, NO_3^- and SO_4^{2-}	1000
Alanine, citric and tartaric acids	100
Glucose, VB_6 and B_{12}	10
Catechol, dopamine, acetaminophen and 4-amino phenol	5
Uric acid	5

calibration curve with the corresponding linear regression equation [I_P (μA) = 2.067 C (μM) + 12.335, R^2 = 0.9959] with a DL of 1.681 μM (Fig. 7B). The sensitivities of the prepared sensor towards AA were virtually the same in the absence (2.066 μA/μM) and presence (2.067μA/μM) of VB_2 that means that the oxidation processes of AA and VB_2 at the PMO/GCE are independent. Similarly, DPVs of VB_2 in the concentration range of 55.0-75.0 μM at a constant 10.0 μM concentration of AA were recorded (Fig. 7C). Plotting the VB_2 anodic peak current versus concentration (Fig. 7D) resulted in a linear curve [I_P (μA) = 0.94 C (μM) + 7.151, R^2 = 0.9963] with a DL of 0.462 μM. These results indicate that the modified electrode can measure AA and VB_2 simultaneously.

Interference Studies

The effects of different foreign species were studied to prove the sensor specificity in determining AA and VB_2. The selectivity of the PMO/GCE was evaluated by determining various common species in0.1 M PBS containing 0.1 mM AA and 0.1 mM of VB_2, individually (see Table 2). The presence of 1000-fold concentration

ratios of various common ions, such as Na^+, K^+, Mg^{2+}, Cl^-, NO_3^- and SO_4^{2-} do not interfere with AA or VB_2 determination. Also, 100-fold of some physiological substances such as alanine, citric and tartaric acids and 10-fold of glucose, VB_6, and B_{12} and 5-fold of catechol, dopamine, acetaminophen, 4-amino phenol, and uric acid leads to a change in the peak current of AA or VB_2 lower than ±5%. Thus, the proposed sensor can measure AA and VB_2 in even complex mixtures.

Reproducibility and Stability Studies

The reproducibility of the PMO/GCE was examined using six successive measurements of 0.1 mM AA and 0.1 mM VB_2 in 0.1 M PBS, individually. The relative standard deviation (RSD) values of 2.84% and 4.5% were obtained for AA and VB_2, respectively (Table 3). The peak currents remain at 93.0% (AA) and 91.14% (VB_2) of their initial values after storing for a month at room temperature, indicating that PMO/GCE is stable in the long term. This study demonstrated the high stability and reproducibility of the modified electrode for VB_2 and AA detection.

Table 3. Reproducibility of PMO/GCE for Measurement of AA and VB_2

Experiment No.	Peak current	
	AA (µA)	VB_2 (µA)
1	6.99	3.84
2	7.062	3.514
3	7.144	3.459
4	7.326	3.441
5	7.471	3.424
6	7.543	3.316
Mean	7.265	3.449
SD	0.2059	0.1579
RSD (%)	2.8	4.5

Real Samples Analysis

To study the applicability of the fabricated electrode in a practical analytical situation, it was tested for the detection of AA in real samples such as (orange, lemon, oral drops and vitamin C tablets) and VB_2 in milk, B-complex syrup and tablets. Herein, the standard addition method was utilized to detect the two analytes through DPVs (Figs. 8A and B) at optimum condition and then recoveries were calculated. The proposed method was in good agreement with reported methods [41-43]. The results of AA and VB_2 determination are depicted in Tables 4 and 5, respectively. Excellent recoveries for all samples were obtained between 97.53% and 102.2%, signifying the high applicability of the PMO/GCE for the detection of AA and/or VB_2 in real samples without any significant interferences from sample matrices.

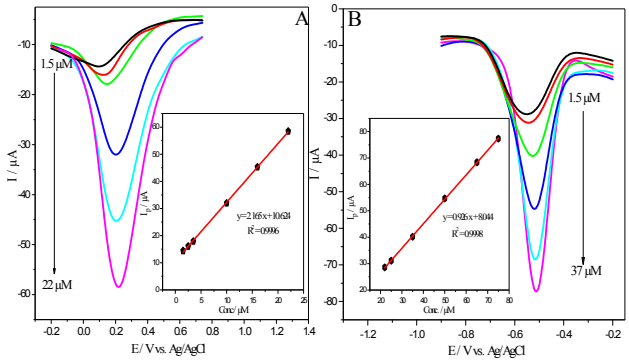

Fig. 8. DPVs of the PMO/GCE (A) in 0.1 M PBS (pH 7.0) with standard added of AA (1.5, 2.5, 3.5, 10.0, 16.0 and 22.0 µM) and (B) in 0.1 M PBS (pH 6.0) with standard added of VB_2 (22.0, 25.0, 35.0, 50.0,65.0 and 75.0 µM) at pulse height 25×10^{-3} V, pulse width 50×10^{-3} s, step time 0.1 s and scan rate 20 mV s^{-1}.

CONCLUSIONS

A simple and cheap electrochemical sensor for the simultaneous determination of AA and VB_2 was successfully constructed. Due to the high electrochemical activity of MO, a polymer film of MO was synthesized on the surface of a GCE electrode using the CV technique. The modified electrode exhibited high sensitivity, low detection limit, good stability, and high anti-interference ability to detect AA and VB_2. The fabricated sensor has been successfully employed to detect AA and VB_2 in various real

Table 4. Detection of AA in Real Samples at the PMO/GCE (n = 3)

Sample	Added (μM)	Found proposed method (μM)	Found proposed method (μM)	Recovery (%)
Tablet	0.0	5.11	5.22	-
	5.0	9.86	-	97.53
Orange	0.0	4.92	5.39	-
	3.0	7.99	8.23	100.88
Lemon	0.0	5.99	5.92	-
	3.0	9.02	8.90	100.33

Table 5. Detection of RF in Real Samples at the PMO/GCE (n = 3)

Sample	Added (μM)	Found proposed method (μM)	Found proposed method (μM)	Recovery (%)
Tablet	0	1.51	1.51	-
	1.0	2.52	2.45	100.4
Milk	0	1.28	1.3	-
	1.0	2.32	2.29	101.75
Syrup	0	3.0	-	-
	2.0	5.11	-	102.2

samples. The obtained results were in statistical compatibility with the data of the alternative reported method. This proved that the proposed method is feasible to be applied without samples pretreatment.

REFERENCES

[1] M.M. Motaghi, H. Beitollahi, S. Tajik, R. Hosseinzadeh, Int. J. Electrochem. Sci. 11 (2016) 7860.

[2] H. Zhu, G. Xu, Int. J. Electrochem. Sci. 12 (2017) 3882.

[3] S.Z. Mohammadi, H. Beitollahi, Z. Dehghan , R. Hosseinzadeh, Appl. Organomet. Chem. 32 (2018) 8.

[4] P. Yomthiangthae, T. Kondo, O. Chailapakul, W. Siangproh, New J. Chem. 44 (2020) 12612.

[5] D.M. Stankovic, D. Kuzmanovic, E. Mehmeti, K. Kalcher, Monatsh Chem. 147 (2016) 1000.

[6] A. Tai, E. Gohda, J. Chromatogr. B 853 (2007) 214.

[7] X. Sun, Y. Niu, S. Bi, S. Zhang, J. Chromatogr. B 870 (2008) 46.

[8] N. Anastos, N.W. Barnett, B.J. Hindson, C.E. Lenehan, S.W. Lewis, Talanta 64 (2004) 130.

[9] A. Tai, J. Takebayashi, A. Ueno, F. Gohda, I. Yamamoto, J. Chromatogr. B 840 (2006) 38.

[10] B.N. Chandrashekar, B.E.K. Swamy, K.J. Gururaj, C. Cheng, J. Mol. Liq. 231 (2017) 379.

[11] R. Thangamuthu, S.M.S. Kumar, K.C. Pillai, Sens. Actuators B Chem. 120 (2007) 745.

[12] S.A. Kumar, P.H. Lo, S.M. Chen, Biosens. Bioelectron. 24 (2008) 518.

[13] S. Thiagarajan, T.H. Tsai, S.M. Chen, Biosens. Bioelectron. 24 (2009) 2712.

[14] A. Kowalczyk, M. Sadowska, B. Krasnodebska-Ostrega, A.M. Nowicka, Talanta 163 (2017) 72.

[15] M. Arvand, A. Pourhabib, M. Giahi, J. Pharm. Anal. 7 (2017) 117.

[16] K. Reddaiah, T.M. Reddy, P. Raghu, J. Electroanal. Chem. 682 (2012) 171.

[17] A.B. Monnappa, J.G.G. Manjunatha, A.S. Bhatt, H.

Nagarajappa, J. Sci. Adv. Mater Dev. 6 (2021) 424.
[18] K. Giribabu, Y. Haldorai, M.Rethinasabapathy, S.C. Jang, R. Suresh, W.S. Cho, Y.K. Han, Ch. Roh, Y.S. Huh, V. Narayanan, Curr. Appl. Phys. 17 (2017) 1119.
[19] V.V. Tkach, J.I.F. de Paiva Martins, Y.G. Ivanushko, P.I. Yagodynets, Bioenterface Res. Appl. Chem. 12 (2022) 4028.
[20] T.E. Chiwunze, V.N. Palakollu, Atal A.S. Gill, F. Kayamba, N.B. Thapliyal, R. Karpoormath, Mater. Sci. Eng. C 97 (2019) 285.
[21] Y. Hong, S. Yuanyuan, L. Xinhua, T. Yuhai, H. Liying, Electrochim. Acta 52 (2007) 6171.
[22] M. Pandurangachar, B.E.K. Swamy, U. Chandra, O. Gilbert, B.S. Sherigara, Int, J. Electrochem. Sci. 4 (2009) 683.
[23] J.E.B. Randles, Trans. Faraday Soc. 44 (1948) 327.
[24] A. Sevcik, Collect. Czech. Chem. Commun. 13 (1948) 349.
[25] A.G.-M. Ferrari, C.W. Foster, P.J. Kelly, D.A.C. Brownson, C.E. Banks, Biosens. 8 (2018) 53.
[26] F. Khaleghi, Z. Arab, V.K. Gupta, M.R. Ganjali, P. Norouzi, N. Atar, M.L. Yola, J. Mol. Liq. 221 (2016) 672.
[27] Sh. Jahani, H. Beitollahi, Anal. Bioanal. Electrochem. 8 (2016) 168.
[28] E. Zarei, M.R. Jamali, J. Bagheri, J. Anal. Chem. 74 (2019) 1222.
[29] E. Mehmeti, D.M. Stanković, S. Chaiyo, Ľ. Švorc, K. Kalcher, Microchim. Acta 183 (2016) 1624.
[30] A. Baghizadeh, H.K. Maleh, Z. Khoshnama, A. Hassankhani, M. Abbasghorbani, Food Anal. Methods 8 (2015) 557.
[31] Z. Taleat, M.M. Ardakani, H. Naeimi, H. Beitollahi, M. Nejati, H.R. Zare, Anal. Sci. August 24 (2008) 1044.
[32] N. Ejhieh, A. Pouladsaz, J. Ind. Eng. Chem. 20 (2014) 2152.
[33] J.C. Miller, J.N. Miller, Statistics for Analytical Chemistry. Ellis Horwood Series, PTR Prentice Hall, London, 1993.
[34] H. Rageh, M. Abdel-sabour, Anal. Bioanal. Electrochem. 9 (2017), 364.
[35] K.P. Aryal, H.K. Jeonga, Chem. Phys. Lett. 757 (2020) 137881.
[36] Lu. Zhang, Int. J. Electro Chem. Sci. 15 (2020) 5057.
[37] D. Banan, W.T. Tan, Y.Sulaiman, M.F. Yusri, M. Zidan, S. AbGhani, Int. J. Electro Chem. Sci. 8 (2013) 12530.
[38] G. Tigari, J.G. Manjunatha, C. Raril, N. Hareesha, Chem. Select 4 (2019) 2173.
[39] T. Nie, J.-K. Xu, L.-M. Lu, K.-X. Zhang, L. Bai, Y.-P. Wen, Biosens. Bioelectron. 50 (2013) 250.
[40] H. Wang, X. Zhang, S. Wang, S. Xiao, H. Ma, X. Wang, Microchem. J. 158 (2020) 105233.
[41] M. Bijad, H.K. Maleh, M.A. Khalilzadeh, Food Anal. Methods 6 (2013) 1647.
[42] E.K. Janghel, S. Sar, Y. Pervez, J. Sci. Ind. Res. 71 (2012) 555.
[43] S.S. Khaloo, S. Mozaffari, P. Alimohammadi, H.K. Joliet Ordookhanian, Int. J. Food Prop. 19 (2016) 2283.